

The DESC Stellarator Code Suite Part II: Perturbation and continuation methods

Rory Conlin,^{a)} Daniel W. Dudt,^{b)} Dario Panici,^{c)} and Egemen Kolemen^{d)}
Princeton University, Princeton, New Jersey 08544

(Dated: March 31, 2022)

ABSTRACT

A new perturbation and continuation method is presented for computing and analyzing stellarator equilibria. The method is formally derived from a series expansion about the equilibrium condition $\mathbf{F} \equiv \mathbf{J} \times \mathbf{B} - \nabla p = 0$, and an efficient algorithm for computing solutions to 2nd and 3rd order perturbations is developed. The method has been implemented in the DESC stellarator equilibrium code, using automatic differentiation to compute the required derivatives. Examples are shown demonstrating its use for computing complicated equilibria, perturbing a tokamak into a stellarator, and performing parameter scans in pressure, rotational transform and boundary shape in a fraction of the time required for a full solution.

I. INTRODUCTION

In the search for controlled nuclear fusion, 3D magnetic confinement devices such as stellarators have been shown to have several advantages over 2D magnetic geometries such as tokamaks, such as lower risk of disruption¹ and current-free steady state operation². However, achieving good performance in a stellarator often requires significant optimization of the plasma equilibrium. An additional advantage is that because of the generally lower plasma current and consequently fewer instabilities, the physics are better understood, and so more of the design and optimization can be done computationally, without requiring building and testing full scale devices³. Despite this, designing and optimizing 3D magnetic equilibria that have good properties is still a computationally intensive task, for which a number of codes and software packages have been developed⁴⁻⁹.

Perturbation methods have been used heavily in tokamak plasma physics, primarily to analyze the stability of axisymmetric MHD equilibria by searching for a perturbation that minimizes the energy of the plasma, as in Bernstein's energy principle¹⁰. This has been extended to a wide range of codes for analyzing fusion devices under small perturbations to an MHD equilibrium, such as the GPEC suite of codes¹¹⁻¹⁴ for analyzing tokamak configurations under 3D perturbations.

Continuation methods have received less attention in the fusion community, though they have seen extensive use in other fields such as^{15,16}. For the purposes of the present work, continuation methods can be used to solve parameterized equations of the form $F(x, \eta) = 0$, where we identify x as the solution vector, and η as a continuation parameter. When η is varied we find a family of solutions connected in parameter space, as well as possible branches and bifurcations of this family, indicated by points where the Jacobian of F is singular. Starting from the initial value (x_0, η_0) where F is zero, we continuously vary η while simultaneously varying x such that the equation $F(x, \eta) = 0$ is satisfied. Various methods exist for finding the solution curve (the locus of points (x, η) where $F(x, \eta) = 0$ is satisfied) such as piecewise linear (simplex) continuation and pseudo-arclength methods¹⁷. In an abstract sense, the standard multigrid method for solving partial differential equations can be thought of as a discrete continuation method, where the continuation parameter η governs the level of numerical resolution (ie grid spacing, number of basis functions etc.)

In general, existing codes for computing stellarator equilibria^{5,7} only find discrete equilibria, and solving for a new equilibrium requires running the code from scratch (possibly with a different starting guess). Several questions that may then be asked are:

1. Can these equilibria be computed more efficiently?
2. Given a single equilibrium solution, can we find other similar solutions?
3. What does the full phase space of 3D MHD equilibria look like?

In this paper, we describe a new continuation method for computing complicated stellarator equilibria using perturbations that attempts to resolve these questions. In [section II](#) we describe the mathematical background to the perturbation method, while in [section III](#) we describe the implementation of the method in the DESC code. In [section IV](#) demonstrate how to use these perturbations in a continuation method for computing stellarator equilibria. In [section V](#) we demonstrate other applications of the perturbation method for computing and analyzing stellarator equilibria.

^{a)} wconlin@princeton.edu

^{b)} ddudt@princeton.edu

^{c)} dpanici@princeton.edu

^{d)} ekolemen@princeton.edu

II. PERTURBATIONS

A general fixed-boundary equilibrium problem can be described by a set of parameters $\mathbf{c} = \{R_b, Z_b, p, \iota, \Psi\}$ where R_b, Z_b are the R, Z coordinates of the boundary surface, p is the pressure profile, ι the rotational transform, and Ψ the total toroidal flux through the torus. In many spectral equilibrium codes^{4,5}, the independent variables that define the equilibrium can be given by $\mathbf{x} = [R_{lmn}, Z_{lmn}, \lambda_{lmn}]$ where R_{lmn}, Z_{lmn} and λ_{lmn} are spectral coefficients of the flux surface positions and the poloidal stream function (indexed by l in the radial direction, m in the poloidal direction, and n in the toroidal direction). The condition of MHD equilibrium can then be written as a (possibly vector valued) nonlinear algebraic equation involving the fixed parameters and independent variables, $\mathbf{f}(\mathbf{x}, \mathbf{c}) = 0$. The function f is the discretized form of the general MHD force balance $\mathbf{J} \times \mathbf{B} - \nabla p = 0$ ⁴, or a condition on the gradient of the energy functional $W = \int_V (B^2/2\mu_0 + p) dV$ ⁵.

Given a set of parameters \mathbf{c} and a solution vector \mathbf{x} which satisfy $\mathbf{f}(\mathbf{x}, \mathbf{c}) = 0$, we wish to find how the equilibrium would change if the parameters \mathbf{c} are perturbed to $\mathbf{c} + \Delta\mathbf{c}$. For instance, we may have a solution for a vacuum equilibrium and want to see how adding finite pressure changes it, or we may start with a 2D tokamak solution and add a 3D perturbation to the boundary shape to form a stellarator.

We assume that the new equilibrium is given by $\mathbf{x} + \Delta\mathbf{x}$, and expand f in a Taylor series^a:

$$\begin{aligned} \mathbf{f}(\mathbf{x} + \Delta\mathbf{x}, \mathbf{c} + \Delta\mathbf{c}) &= \mathbf{f}(\mathbf{x}, \mathbf{c}) + \frac{\partial \mathbf{f}}{\partial \mathbf{x}} \Delta\mathbf{x} + \frac{\partial \mathbf{f}}{\partial \mathbf{c}} \Delta\mathbf{c} + \frac{1}{2} \frac{\partial^2 \mathbf{f}}{\partial \mathbf{x}^2} \Delta\mathbf{x} \Delta\mathbf{x} \\ &+ \frac{1}{2} \frac{\partial^2 \mathbf{f}}{\partial \mathbf{c}^2} \Delta\mathbf{c} \Delta\mathbf{c} + \frac{\partial^2 \mathbf{f}}{\partial \mathbf{x} \partial \mathbf{c}} \Delta\mathbf{x} \Delta\mathbf{c} + \dots \quad (1) \end{aligned}$$

We wish to solve this equation for $\Delta\mathbf{x}$ such that $\mathbf{f}(\mathbf{x} + \Delta\mathbf{x}, \mathbf{c} + \Delta\mathbf{c}) = 0$. At first order this is a straightforward algebraic equation, but at higher orders it becomes a tensor polynomial equation which can be difficult or impossible to solve efficiently (for example, if \mathbf{f} is a vector valued function, just storing the 2nd derivative tensor in memory could require upwards of 100 GB). Instead of seeking a direct solution, we can try a perturbative approach, were we introduce an arbitrary small parameter ϵ and further expand $\Delta\mathbf{x}$ and $\Delta\mathbf{c}$ in a perturbation series

in powers of ϵ (we assume that $\Delta\mathbf{c}$ is known a-priori and so only a first order term is required).

$$\Delta\mathbf{x} = \epsilon \mathbf{x}_1 + \epsilon^2 \mathbf{x}_2 + \dots \quad (2)$$

$$\Delta\mathbf{c} = \epsilon \mathbf{c}_1 \quad (3)$$

$$(4)$$

Plugging this into Equation 1 (and setting $\mathbf{f}(\mathbf{x}, \mathbf{c}) = \mathbf{f}(\mathbf{x} + \Delta\mathbf{x}, \mathbf{c} + \Delta\mathbf{c}) = 0$) we get:

$$\begin{aligned} 0 &= \frac{\partial \mathbf{f}}{\partial \mathbf{x}} (\epsilon \mathbf{x}_1 + \epsilon^2 \mathbf{x}_2) + \frac{\partial \mathbf{f}}{\partial \mathbf{c}} \epsilon \mathbf{c}_1 + \frac{1}{2} \frac{\partial^2 \mathbf{f}}{\partial \mathbf{x}^2} (\epsilon \mathbf{x}_1 + \epsilon^2 \mathbf{x}_2) (\epsilon \mathbf{x}_1 + \epsilon^2 \mathbf{x}_2) \\ &+ \frac{1}{2} \frac{\partial^2 \mathbf{f}}{\partial \mathbf{c}^2} \epsilon \mathbf{c}_1 \epsilon \mathbf{c}_1 + \frac{\partial^2 \mathbf{f}}{\partial \mathbf{x} \partial \mathbf{c}} (\epsilon \mathbf{x}_1 + \epsilon^2 \mathbf{x}_2) \epsilon \mathbf{c}_1 + h.o.t. \quad (5) \end{aligned}$$

We can then collect powers of ϵ and set each order of ϵ to zero in turn. The first order equation gives:

$$0 = \frac{\partial \mathbf{f}}{\partial \mathbf{x}} \epsilon \mathbf{x}_1 + \frac{\partial \mathbf{f}}{\partial \mathbf{c}} \epsilon \mathbf{c}_1 \quad (6)$$

$$\mathbf{x}_1 = - \left(\frac{\partial \mathbf{f}}{\partial \mathbf{x}} \right)^{-1} \left(\frac{\partial \mathbf{f}}{\partial \mathbf{c}} \mathbf{c}_1 \right) \quad (7)$$

The second order term gives:

$$\begin{aligned} 0 &= \frac{\partial \mathbf{f}}{\partial \mathbf{x}} \epsilon^2 \mathbf{x}_2 + \frac{1}{2} \frac{\partial^2 \mathbf{f}}{\partial \mathbf{x}^2} \epsilon^2 \mathbf{x}_1 \mathbf{x}_1 + \frac{1}{2} \frac{\partial^2 \mathbf{f}}{\partial \mathbf{c}^2} \epsilon^2 \mathbf{c}_1 \mathbf{c}_1 + \frac{\partial^2 \mathbf{f}}{\partial \mathbf{x} \partial \mathbf{c}} \epsilon^2 \mathbf{x}_1 \mathbf{c}_1 \\ \mathbf{x}_2 &= - \left(\frac{\partial \mathbf{f}}{\partial \mathbf{x}} \right)^{-1} \left(\frac{1}{2} \frac{\partial^2 \mathbf{f}}{\partial \mathbf{x}^2} \mathbf{x}_1 \mathbf{x}_1 + \frac{1}{2} \frac{\partial^2 \mathbf{f}}{\partial \mathbf{c}^2} \mathbf{c}_1 \mathbf{c}_1 + \frac{\partial^2 \mathbf{f}}{\partial \mathbf{x} \partial \mathbf{c}} \mathbf{x}_1 \mathbf{c}_1 \right) \end{aligned}$$

In general, the second derivative terms will be large, dense, rank 3 tensors (recall that \mathbf{f} can be a vector valued function), which may be extremely expensive to compute and may not even fit in memory for high resolution cases. However, it is important to note that the full second derivatives are never needed (or indeed full first derivatives apart from the Jacobian matrix $\partial \mathbf{f} / \partial \mathbf{x}$). All that is needed are directional derivatives or Jacobian vector products. In the DESC code (section III) these are calculated using forward mode automatic differentiation at a cost a few times greater than the cost of a single evaluation of \mathbf{f} . These terms could also be approximated using finite differences at a similar cost. This means that at each order the most expensive operation is solving a linear system of the form

$$\mathbf{J} \mathbf{x}_i = \mathbf{b} \quad (8)$$

where $\mathbf{J} \equiv \partial \mathbf{f} / \partial \mathbf{x}$ is the Jacobian matrix and is the same at each order, so only needs to be decomposed once and i is the order of the term in the perturbation series. Because of these computation and memory savings, the method has been extended to 3rd order in the DESC code (see section III), though in most situations 1st or 2nd order perturbations gives acceptable results (see Figure 2).

^a Some care must be taken here, as we are implicitly assuming that the function f is at least C^2 continuous. The DESC code assumes the existence of nested flux surfaces so that there is an analytic mapping between real space and magnetic coordinates. In cases where the assumption of nested surfaces is violated, this mapping may not exist. However, we note that the force balance equations are still analytic functions of the dependent variables (it can be shown that they form a high order polynomial), though their physical meaning will be somewhat unclear in regions where nested surfaces don't exist

It is instructive to note that the first order term in the perturbation series for $\Delta\mathbf{x}$ is effectively the Newton step, while the second order term is commonly referred to as the Halley step in optimization literature^{18,19}. While Newton’s method converges quadratically²⁰ when started sufficiently close to a solution, if started far away it may diverge and so in practice the method must be globalized using either a line search or a trust region framework. Although we assume that we begin near or at an equilibrium so that $\mathbf{f}(\mathbf{x}, \mathbf{c}) = 0$, depending on the size of the perturbation the solution landscape may change such that this is no longer the case, and we find in practice in several cases the unconstrained Newton step causes the solution to diverge. There is also an additional constraint inherent in the approach taken that the second order term should be smaller than the first order term by a factor $\epsilon \ll 1$.

This suggests that a natural way to enforce these conditions and ensure reasonable convergence properties is to use a trust region method. When expanding the objective function in a Taylor series we are effectively approximating it by a linear or quadratic function. Instead of seeking the global minimizer to these model functions, the trust region approach instead recognizes that the Taylor approximation is only valid in some small neighborhood and restricts the step size accordingly. Mathematically, instead of finding the exact solution \mathbf{x}_i^* to the linear system

$$\mathbf{J}\mathbf{x}_i = \mathbf{b} \quad (9)$$

We instead seek a solution to the following optimization problem:

$$\min_{\mathbf{x}_i} \|\mathbf{J}\mathbf{x}_i - \mathbf{b}\|^2 \quad s.t. \quad \|\mathbf{x}_i\| \leq r \quad (10)$$

where r is the radius of the trust region. This subproblem has two possible solutions²⁰: either the true solution \mathbf{x}_i^* lies within the trust region, or else that there is a scalar $\alpha > 0$ such that

$$(\mathbf{J} + \alpha I)\mathbf{x}_i = \mathbf{b}, \quad \|\mathbf{x}_i\| = r \quad (11)$$

The constrained value for \mathbf{x}_i is efficiently found using a 1D root finding method in α , in the DESC code we use a bracketed Newton method. The cost of solving this subproblem is roughly the cost of one singular value decomposition of the Jacobian \mathbf{J} , or two to three Cholesky factorizations of the approximate Hessian matrix $\mathbf{B} \equiv \mathbf{J}^T \mathbf{J}$.

Selection of the trust region radius r is traditionally done adaptively within an optimization loop, by comparing the actual reduction in the residual at each step with that predicted by the model function. In a perturbation, only a single “step” is taken, and we have found empirically that setting the trust region at a small fraction of $\|\mathbf{x}\|$ generally gives good results, typically $r = 0.1\|\mathbf{x}\|$. For second and higher order perturbations, such a large trust region can result lead to inaccurate results. This

can be understood by considering the expansion made in Equation 2, where it was implicitly assumed that the 2nd order correction was a factor of ϵ smaller than the first order term. Using a large trust region for the first order term ($r = 0.1\|\mathbf{x}\|$) and a smaller trust region for the higher order terms correctly enforces this assumed scaling. In practice we obtained good performance using $r_i = 0.1\|\mathbf{x}_i\|$, so the second order term is an order of magnitude less than the first order term and so on for higher orders.

III. THE DESC CODE

DESC is a recently developed⁴ pseudo-spectral code for computing 3D MHD equilibria. DESC computes 3D MHD equilibria by solving the force balance equations $\mathbf{J} \times \mathbf{B} - \nabla p = 0$ as opposed to the more common variational method which minimizes the MHD energy $\int_V (B^2/2\mu_0 + p) dV$. The independent variables in the equation are the positions of the flux surfaces (R, Z) as well as the stream function λ , defined as the difference between the boundary poloidal angle θ and the straight field line poloidal angle: $\vartheta = \theta + \lambda$. These quantities are discretized in a Fourier-Zernike basis, using a Fourier series in the toroidal direction and Zernike polynomials in the poloidal/radial directions. After discretization, the equilibrium equation is expressed as a set of nonlinear algebraic equations $\mathbf{f}(\mathbf{x}, \mathbf{c}) = 0$ where \mathbf{x} is a vector containing the spectral coefficients of R, Z , and λ , while \mathbf{c} contains fixed parameters that define the equilibrium problem, such as the pressure and rotational transform profiles and the fixed boundary shape.

Since it’s original publication⁴, DESC has undergone a major upgrade that involved porting it from MATLAB to Python in order to take advantage of the JAX library²¹ for automatic differentiation (AD) and just-in-time (JIT) compilation. Initially developed for machine learning applications, JAX provides an NumPy^{22,23}-like API for common mathematical operations and allows arbitrary functions to be differentiated using forward or reverse mode AD. This allows the calculation of exact derivatives of the objective function automatically, rather than having to code them by hand which is time-consuming and error prone, or using finite differences which are computationally expensive and can be inaccurate. It is also much more flexible as new objective functions can be added and optimized by defining only the forward pass, which is of great use in stellarator optimization where new objectives may be added in the future. JAX also allows for JIT compiling of code to both CPUs and GPUs which significantly speeds up calculation, approaching speeds of traditional compiled languages, avoiding one of the primary limitations of Python for scientific computing. Additionally, given that the vast majority of new supercomputers heavily leverage GPUs, and this trend is likely to continue, using JAX allows DESC to take full advantage of all the compute capability available, rather

than being limited to CPU-only parallelization like many legacy codes. This allows a "best of both worlds" approach where the code is easy to use, maintain, adapt, and upgrade, while still being fast enough for production applications.

Transitioning the code to Python also entailed refactoring the code to a more object-oriented style that helps to keep things modular and extensible, allowing new objectives to be defined by composing simpler predefined operations. The code has been designed to make extending it to add new functionality as easy as possible, and work is currently underway on allowing the computation of free boundary equilibria, combined coil/plasma optimization, as well as optimization for physics targets like quasisymmetry and particle confinement. Details on these improvements will be the subject of future works.

Several aspects also make DESC the ideal code for implementing the perturbation method outlined in [section II](#):

1. Using a pseudo-spectral discretization significantly reduces the number of independent variables, resulting in smaller Jacobian matrices.
2. Using JAX allows fast and accurate computation of the required derivatives and Jacobian-vector products.
3. Formulating the equilibrium problem as a system of nonlinear equations means the first order perturbation term spans the entire tangent space at the initial point (assuming the Jacobian is full rank), rather than just the single line along the gradient of a scalar objective function.

In addition, formulating the problem as a system of nonlinear equations and solving them in a least squares sense also effectively gives an extra order of derivative for free. This can be seen by considering the least squares problem

$$\min_{\mathbf{x}} y(\mathbf{x}) \equiv \frac{1}{2} \mathbf{f}(\mathbf{x})^T \mathbf{f}(\mathbf{x}) \quad (12)$$

where \mathbf{f} is a vector valued function, and y is the sum of squares of the residuals of \mathbf{f} . The gradient of y is given by

$$\frac{dy}{d\mathbf{x}} = \mathbf{f}^T \frac{d\mathbf{f}}{d\mathbf{x}} \quad (13)$$

and its Hessian (matrix of second partial derivatives) is given by

$$\frac{d^2y}{d\mathbf{x}^2} = \frac{d\mathbf{f}^T}{d\mathbf{x}} \frac{d\mathbf{f}}{d\mathbf{x}} + \mathbf{f}^T \frac{d^2\mathbf{f}}{d\mathbf{x}^2} \quad (14)$$

Given that \mathbf{f} is the function we are trying to minimize in the least squares sense, we can generally assume that the 2nd term in the Hessian is negligible compared to

the first, the so-called "small residual approximation"²⁰. This gives an approximate Hessian $\frac{d^2y}{d\mathbf{x}^2} \sim \frac{d\mathbf{f}^T}{d\mathbf{x}} \frac{d\mathbf{f}}{d\mathbf{x}}$, meaning that using only first derivative information about \mathbf{f} gives us both first and second derivative information about y . In addition, the approximate Hessian this gives is always positive semi-definite, leading to a convex subproblem which is easy to solve.

IV. CONTINUATION METHOD

Many MHD equilibrium codes⁵⁷ use a multigrid approach, where an initial guess is specified on a coarse grid, and the error is minimized on that grid before being interpolated to a finer grid and re-solved, continuing until the finest resolution level has been reached. This is done both to speed computation by doing more calculations on coarser grids, and also to make it more robust to poor initial guesses and avoid additional saddle points that can appear in high dimensional spaces²⁴. DESC offers this as well, allowing the resolution to be varied in the radial, poloidal, and toroidal directions independently.

In addition to the standard multigrid approach, DESC has also implemented a new continuation method using the perturbation techniques described in [section II](#). In general, continuation methods seek to find how the solution to an equation varies as parameters are changed. Using the notation of [section II](#) we can view \mathbf{x} to be an implicit function of \mathbf{c} , related by the constraint equation $\mathbf{f}(\mathbf{x}, \mathbf{c}) = 0$, and try to find the map that relates \mathbf{x} and \mathbf{c} along lines of $\mathbf{f}(\mathbf{x}, \mathbf{c}) = 0$.

In this work, we note two properties that make continuation methods especially relevant:

1. 2D (axisymmetric) equilibria are much easier to compute than 3D equilibria, due to the guaranteed existence of flux surfaces in axisymmetric equilibria, and the significant reduction in the number of variables needed to represent the solution.
2. Vacuum (vanishing beta) equilibria are easier to compute than finite pressure equilibria, due to the lack of Shafranov shift.

We can take advantage of these properties to compute complicated stellarator equilibria by first solving an "easy" problem, and then introduce a continuation parameter that transforms our initial solution into the solution to a "hard" problem.

To do this, we introduce 2 scalar continuation parameters: η_b , a multiplier on all of the non-axisymmetric boundary modes, and η_p , a scaling factor for the pressure profile. Setting $\eta_b = 0$ would give a 2D axisymmetric boundary that is "close" to the desired 3D equilibrium, while setting $\eta_p = 0$ would give the vacuum equilibrium with the desired boundary shape. By varying these two parameters, we find a "family" of solutions that are connected continuously.

To vary the parameters, we apply perturbations as outlined in [section II](#). A standard method for solving continuation problems, known as "natural parameter continuation" would be analogous to a 0th order perturbation followed by several Newton iterations, while a first order perturbation would be similar to Gauss-Newton continuation. The higher order perturbations discussed above do not seem to have been explored in the more general continuation method literature, but can be seen as a version of Halley's method applied to the combined system.

In most traditional continuation methods, the step size in the continuation parameter is determined adaptively based on local error estimates and the ratio of predicted to achieved error reduction. In practice we have found that this is often not necessary, and fixing the step sizes a-priori provides sufficiently accurate results. In most cases going from a vacuum equilibrium to a moderate beta of $\sim 3\%$ can be done in a single step, and boundary perturbations in anywhere from 1-4 steps, depending on the desired accuracy and complexity of the boundary. This does require the user to specify the desired perturbation steps explicitly, though a future upgrade to the code is planned to allow adaptive perturbations where the user need only supply an initial guess and the final desired parameters.

As a first example ([Figure 1](#)), we solve for a vacuum heliotron by first solving for a simple circular tokamak, then applying a 3D perturbation to the boundary. After the perturbation, a small number (usually 5-10) of regular Newton iterations are applied to ensure convergence.

Similarly, when computing finite pressure equilibria it can be difficult to estimate the Shafranov shift a-priori for generating a good initial guess. DESC avoids this by first computing a vacuum solution, for which a good initial guess can generally be found by simply scaling the boundary surface. The finite pressure is then added back in as a perturbation, which then often only requires a small number of further iterations to reach convergence as shown in [Figure 2](#).

Perturbation order	Normalized force error ($ F / \nabla p $)
1st order	87.6%
2nd order	29.6%
3rd order	9.7%

Table I: Normalized force balance error vs perturbation order for a pressure increase from $\beta = 0\%$ to $\beta = 3\%$.

While in general the two parameters could be varied in any order, or simultaneously when solving for a 3D finite-beta equilibrium, we have found that first varying η_p , followed by η_b to be more efficient. Varying η_p while holding η_b fixed at 0 allows the pressure perturbations to be done on a 2D axisymmetric configuration, which reduces the computational cost and ensures the existence of good flux surfaces. After reaching a high resolution finite-beta axisymmetric equilibrium, 3D modes are added to the basis functions and the boundary is perturbed to give the final desired 3D finite-beta equilibrium.

This procedure is demonstrated in [Figure 3](#), where the initial solution is an axisymmetric vacuum tokamak. The pressure is then increased, as demonstrated by the Shafranov shift, followed by 3D deformation of the boundary shape to arrive at a W7X like configuration. After each large perturbation, a small number of regular Newton iterations are performed to ensure that an equilibrium has been reached (recall that in the derivation of the perturbations, it was assumed that the initial state before perturbing was an equilibrium). This method was also used to compute the solutions shown in Part I, where a detailed analysis of the force error is given.

An important feature to note about the aforementioned continuation method is that the solution at each step is in fact the "exact" solution to the equilibrium problem with perturbed parameters, and is hence still a valid equilibrium that satisfies MHD force balance and may have desirable physics properties worth studying that may be absent in the final solution. By applying different perturbations and varying different parameters, one can explore whole families of solutions that are "nearby" to a starting equilibrium.

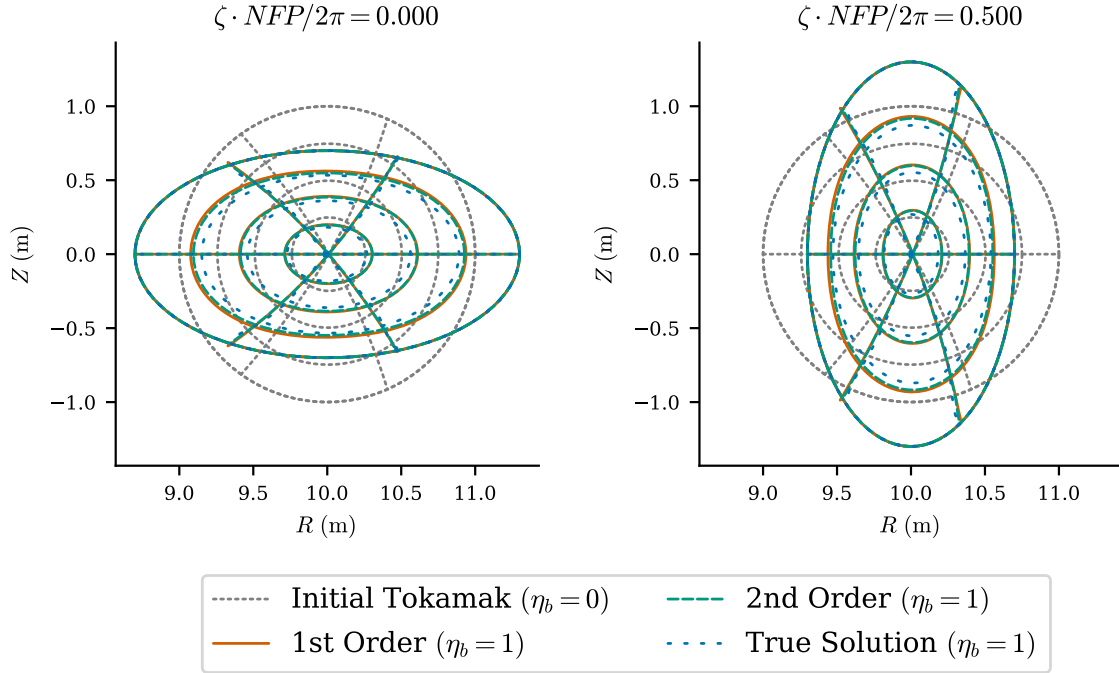


Figure 1: Comparison of perturbed tokamak equilibrium vs true solution for a heliotron like stellarator. The initial tokamak (grey) is axisymmetric. By applying a perturbation (1st order in red, 2nd order in green) to the non-axisymmetric boundary modes, we obtain an approximation to the true 3D solution (blue), obtained by solving from the start with the full 3D boundary shape. The first order perturbation captures the majority of the differences between the initial and true solutions. The second order effects bring the perturbed solution even closer to the true one.

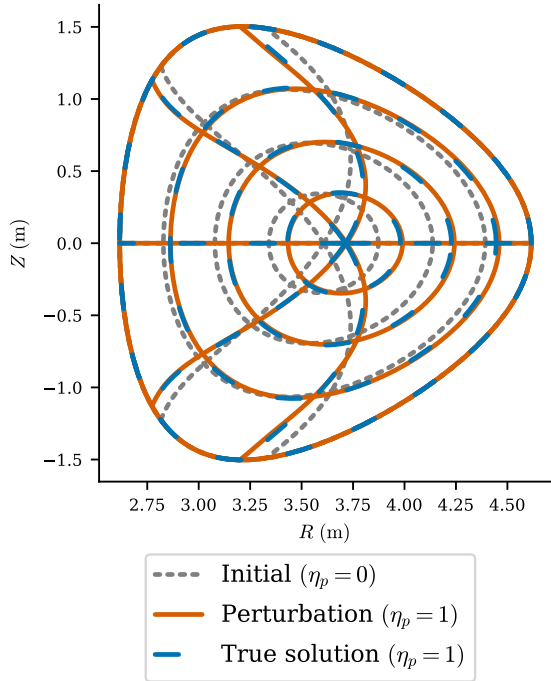


Figure 2: Comparison of perturbed equilibrium vs true solution for a change in pressure from $\beta = 0\%$ to $\beta = 3\%$. The first order perturbation (red) captures the majority of the differences between the initial (grey) and true (blue) solutions. Second and third order effects (not shown for clarity) are visually very similar but significantly reduce the resulting force balance error as shown in [Table I](#).

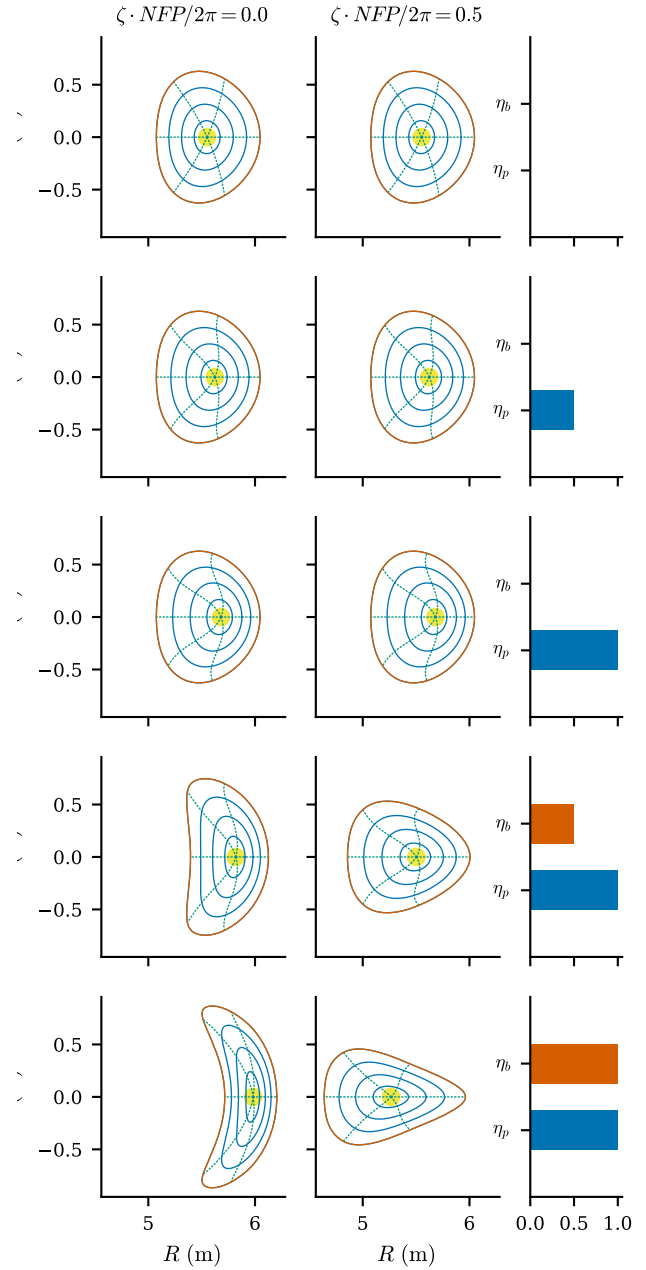


Figure 3: Continuation solution for W7X like equilibrium. Starting from a vacuum 2D equilibrium, the pressure is increased to $\beta \sim 3\%$ in a series of two steps. Then a 3D perturbation is applied to the boundary, broken up into 4 steps (2 shown) to arrive at the final finite β 3D solution.

V. OTHER APPLICATIONS

A. Parameter Scans

Another important feature of continuation methods is revealing how solutions change as parameters of the problem are varied. In the previous section we used this to find single equilibria, but the method can also be used to explore families of equilibria related by a parameter or group of parameters. In this, we find equilibria "nearby" to an equilibrium already found, such as examining the same boundary shape at different values of β or boundary perturbations of varying magnitude and shape such as resonant magnetic perturbations (RMP) in a tokamak. Traditionally this requires re-solving the equilibrium for each new value of the parameter. An alternative approach is to apply a perturbation to an initial equilibrium and find the corresponding changes in the flux surfaces. After applying the first perturbation, we re-linearize about the new state and perturb again, and so step through different equilibria for the cost of a single linear system solve at each step. This represents a significant computational savings compared to solving the full nonlinear problem for each value of the parameter.

Figure 4 shows the flux surfaces on the $\zeta = 0$ and $\zeta = \pi$ plane for a helical stellarator for the same pressure profile scaled to different values of β . The initial solution was at $\beta = 0\%$, and 2nd order perturbations were applied sequentially to step the pressure up to $\beta = 10\%$. The flux surfaces are indistinguishable from those obtained by solving from scratch at each value of β , and the computational cost is significantly reduced, as shown in Table II. Performing such a scan requires only a few lines of code, as shown in Listing 1.

```

1 import numpy as np
2 import desc.io
3 from desc.equilibrium import EquilibriaFamily
4 eq0 = desc.io.load("heliotron_vacuum_solution.h5")[-1]
5 eqf = EquilibriaFamily(eq0)
6 # this corresponds to a change in beta of ~1%
7 dp = np.array([ 1800., 0., -3600., 0., 1800.])
8 for i in range(10):
9     eqf.append(eqf[-1].perturb(dp=dp, order=1))
10    # polish off solution
11    eqf[-1].solve(maxiter=5)

```

Listing 1: Code example for β scan

As another example (Figure 5), a D-shaped tokamak was used as the starting point for variations in the rotational transform profile. The initial equilibrium had a rotational transform on axis of $\iota_0 = 1$, and perturbations were applied to reduce this down to $\iota_0 = 0.34$. As the rotational transform is decreased, we see increased Shafranov shift and deformation of the flux surfaces as the reduced poloidal field struggles to contain the pressure ($\beta \sim 3\%$ in this example).

As in the pressure scan example, the solution obtained by perturbation is indistinguishable by eye from the solution obtained by solving the full equilibrium prob-

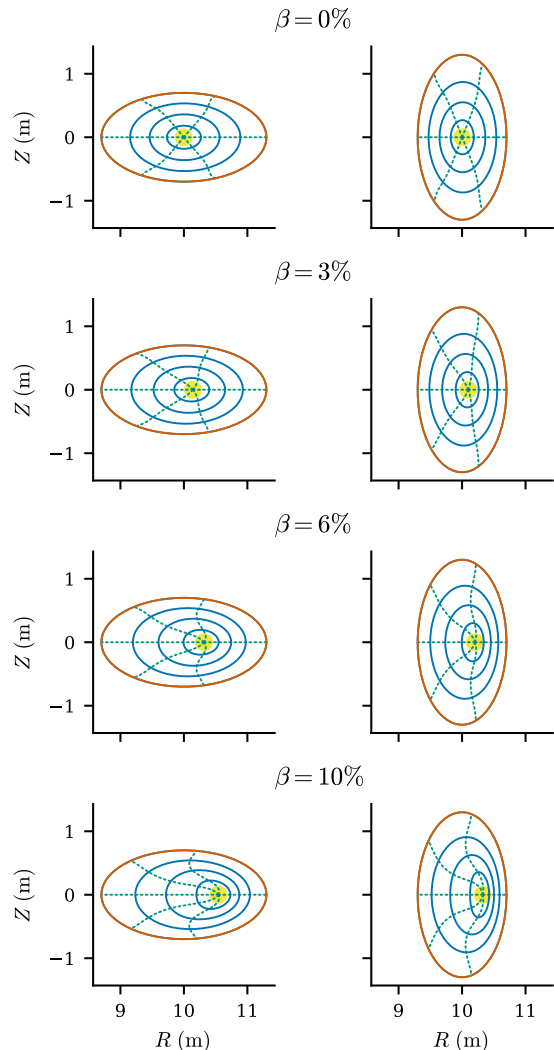


Figure 4: Flux surfaces on the $\zeta = 0$ and $\zeta = \pi$ planes for a helical stellarator. The initial equilibrium had $\beta = 0\%$, and a series of 2nd order perturbations were applied to increase the pressure rather than solving a new equilibrium from scratch each time.

lem, and significantly faster. Once an initial equilibrium is solved, parameter scans can be performed an order of magnitude faster using perturbations than other approaches which require a full solution at each step. The code to perform such a scan is shown in Listing 2.

```

12 import numpy as np
13 import desc.io
14 eq0 = desc.io.load("DSHAPE.h5")[-1]
15 # perturbing a 2nd order polynomial basis for
16 # iota
17 di = np.array([-0.33, 0, 0.33])
18 eq1 = eq0.perturb(di=di, order=2)
19 eq1.solve(maxiter=5)
20 eq2 = eq1.perturb(di=di, order=2)
21 eq2.solve(maxiter=5)

```

Listing 2: Code example for perturbing iota profile

β	Time (s)	
	without perturbations	with perturbations
1	164	78.0
2	174	16.3 s
3	164	14.4 s
4	122	12.6 s
5	127	17.8 s
6	122	19.1 s
7	121	15.2 s
8	134	13.6 s
9	140	16.0 s
10	138	18.3 s
Total	23.4 min	3.68 min

Table II: Computation times for different values of β in the pressure scan shown in Figure 4, both with and without perturbations, starting from a vacuum solution. The first perturbation takes longer as the time includes JIT compilation for the specific problem being solved, resulting in significantly faster times for the subsequent perturbation steps which reuse the same compiled code. All computation done on an AMD Ryzen 7 PRO 4750U with 32 GB memory.

B. Optimization

The perturbation techniques described previously can also be adapted for optimization, where instead of choosing a particular change in the parameters $\Delta\mathbf{c}$ we instead let $\Delta\mathbf{c}$ be a free parameter that is chosen to minimize a cost function $\mathbf{g}(\mathbf{x}, \mathbf{c})$, such as quasisymmetry error^{2,25}, coil complexity^{26–28}, or fast particle confinement^{29,30}:

$$\Delta\mathbf{c}^* = \arg \min_{\Delta\mathbf{c}} \mathbf{g}(\mathbf{x} + \Delta\mathbf{x}, \mathbf{c} + \Delta\mathbf{c}) \quad s.t. \quad \mathbf{f}(\mathbf{x} + \Delta\mathbf{x}, \mathbf{c} + \Delta\mathbf{c}) = 0 \quad (15)$$

Where as before $\Delta\mathbf{x}$ is an implicit function of $\Delta\mathbf{c}$.

This finds the perturbation that most decreases the cost function \mathbf{g} while maintaining force balance, without the need for additional equilibrium solves, and is analogous to a Newton method applied to the objective $\mathbf{g}(\mathbf{x}, \mathbf{c})$ and its constraints $\mathbf{f}(\mathbf{x}, \mathbf{c}) = 0$. In the optimization literature, this is part of a more general class of methods for constrained optimization. Like the perturbations described in section II, this method can also be extended to higher order. This extension and further details on this method of optimization and applications to quasisymmetry will be given in Part III.

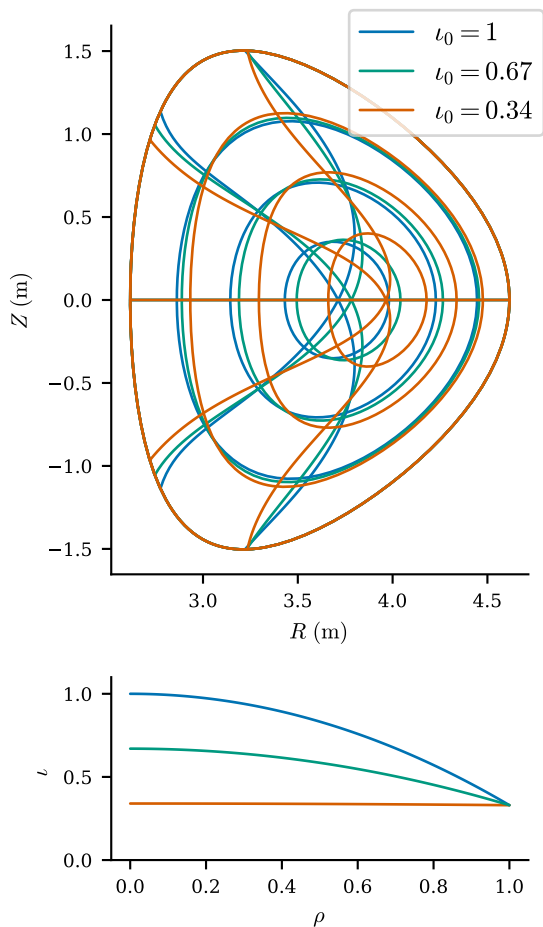


Figure 5: **Top:** Flux surfaces on the $\zeta = 0$ plane for a D-shaped tokamak with varying axis rotational transform. The initial equilibrium (blue) corresponds to $\iota_0 = 1$, and perturbations were used to reduce the axis rotational transform without recomputing the entire equilibrium solution. **Bottom:** Rotational transform profiles corresponding to flux surfaces shown above.

VI. CONCLUSIONS

We have demonstrated a new technique for computing stellarator equilibria, and for exploring how those equilibria change as parameters are varied. The methods are computationally efficient, and offer significant speedups compared to existing techniques, and in many cases offer possibilities that have not existed before. An important future application of these methods is in exploring the connections between different classes of equilibria, such as how tokamaks bifurcate into stellarators, and how different classes of quasisymmetric stellarators may be related.

ACKNOWLEDGEMENTS

This work was supported by the U.S. Department of Energy under contract numbers DE-AC02-09CH11466, DE-SC0022005 and Field Work Proposal No. 1019. The United States Government retains a non-exclusive, paid-up, irrevocable, world-wide license to publish or reproduce the published form of this manuscript, or allow others to do so, for United States Government purposes.

REFERENCES

REFERENCES

- ¹P. Helander, C. D. Beidler, T. M. Bird, M. Drevlak, Y. Feng, R. Hatzky, F. Jenko, R. Kleiber, J. H. Proll, Y. Turkin, and et al., “Stellarator and tokamak plasmas: A comparison,” *Plasma Physics and Controlled Fusion* **54**, 1–33 (2012).
- ²P. Helander, “Theory of plasma confinement in non-axisymmetric magnetic fields,” *Reports on Progress in Physics* **77** (2014), 10.1088/0034-4885/77/8/087001.
- ³A. H. Boozer, “Stellarator design,” *Journal of Plasma Physics* **81** (2015), 10.1017/S0022377815001373.
- ⁴D. Dudt and E. Kolemen, “Desc: A stellarator equilibrium solver,” *Physics of Plasmas* **27**, 102513 (2020).
- ⁵S. P. Hirshman and J. C. Whitson, “Steepest-descent moment method for three-dimensional magnetohydrodynamic equilibria,” *Physics of Fluids* **26**, 3553–3568 (1983).
- ⁶M. Landreman, B. Medasani, F. Wechsung, A. Giuliani, R. Jorge, and C. Zhu, “Simspt: A flexible framework for stellarator optimization,” *Journal of Open Source Software* **6**, 3525 (2021).
- ⁷S. R. Hudson, R. L. Dewar, M. J. Hole, and M. McGann, “Non-axisymmetric, multi-region relaxed magnetohydrodynamic equilibrium solutions,” *Plasma Physics and Controlled Fusion* **54**, 014005 (2012).
- ⁸D. A. Spong, S. P. Hirshman, J. C. Whitson, D. B. Batchelor, B. A. Carreras, V. E. Lynch, and J. A. Rome, “J* optimization of small aspect ratio stellarator/tokamak hybrid devices,” *Physics of Plasmas* **5**, 1752–1758 (1998).
- ⁹M. Drevlak, C. D. Beidler, J. Geiger, P. Helander, and Y. Turkin, “Optimisation of stellarator equilibria with rose,” *Nuclear Fusion* **59** (2019), 10.1088/1741-4326/aaed50.
- ¹⁰I. Bernstein, E. Frieman, M. D. Kruskal, and R. M. Kulsrud, “An energy principle for hydromagnetic stability problems,” *Proceedings of the Royal Society of London. Series A. Mathematical and Physical Sciences* **244**, 17–40 (1958), citation Key: Bernstein1958.
- ¹¹A. H. Glasser, “The direct criterion of newcomb for the ideal mhd stability of an axisymmetric toroidal plasma,” *Physics of Plasmas* **23**, 072505 (2016), citation Key: Glasser2016.
- ¹²A. Glasser, E. Kolemen, and A. H. Glasser, “A riccati solution for the ideal mhd plasma response with applications to real-time stability control,” *Physics of Plasmas* **25**, 032507 (2018), citation Key: Glasser2018.
- ¹³J. K. Park, A. H. Boozer, and A. H. Glasser, “Computation of three-dimensional tokamak and spherical torus equilibria,” *Physics of Plasmas* **14**, 0–9 (2007).
- ¹⁴J.-k. Park, A. H. Boozer, J. E. Menard, A. M. Garofalo, M. J. Schaffer, S. M. Kaye, S. P. Gerhardt, and S. A. Sabbagh, “Importance of plasma response to nonaxisymmetric perturbations in tokamaks,” *Phys. Plasmas* , 12 (2009).
- ¹⁵J. S. Howell, “Computation of viscoelastic fluid flows using continuation methods,” *Journal of Computational and Applied Mathematics* **225**, 187–201 (2009).
- ¹⁶S. L. Richter and R. A. DeCarlo, “Continuation methods: Theory and applications,” *IEEE Transactions on Systems, Man, and Cybernetics* , 459–464 (1983).
- ¹⁷E. L. Allgower and K. Georg, *Numerical Continuation Methods: An Introduction* (Springer-Verlag, Berlin, Heidelberg, 1990).
- ¹⁸W. Gander, “On halley’s iteration method,” *The American Mathematical Monthly* **92**, 131–134 (1985).
- ¹⁹G. Gundersen and T. Steihaug, “On large-scale unconstrained optimization problems and higher order methods,” *Optimization Methods and Software* **25**, 337–358 (2010).
- ²⁰J. Nocedal and S. Wright, *Numerical optimization* (Springer Science & Business Media, 2006).
- ²¹J. Bradbury, R. Frostig, P. Hawkins, M. J. Johnson, C. Leary, D. Maclaurin, G. Necula, A. Paszke, J. VanderPlas, S. Wanderman-Milne, and Q. Zhang, “JAX: composable transformations of Python+NumPy programs,” (2018).
- ²²S. Van Der Walt, S. C. Colbert, and G. Varoquaux, “The numpy array: A structure for efficient numerical computation,” *Computing in Science and Engineering* **13**, 22–30 (2011), arXiv: 1102.1523.
- ²³C. R. Harris, K. J. Millman, S. J. van der Walt, R. Gommers, P. Virtanen, D. Cournapeau, E. Wieser, J. Taylor, S. Berg, N. J. Smith, and et al., “Array programming with numpy,” *Nature* **585**, 357–362 (2020), arXiv: 2006.10256 publisher: Springer US.
- ²⁴Y. Dauphin, R. Pascanu, C. Gulcehre, K. Cho, S. Ganguli, and Y. Bengio, “Identifying and attacking the saddle point problem in high-dimensional non-convex optimization,” *arXiv:1406.2572 [cs, math, stat]* (2014), arXiv: 1406.2572.
- ²⁵A. H. Boozer, “Transport and isomorphic equilibria,” *Physics of Fluids* **26**, 496–499 (1983).
- ²⁶C. Zhu, S. R. Hudson, Y. Song, and Y. Wan, “New method to design stellarator coils without the winding surface,” *Nuclear Fusion* **58** (2018), 10.1088/1741-4326/ab98f2.
- ²⁷C. Zhu, S. R. Hudson, S. A. Lazerson, Y. Song, and Y. Wan, “Hessian matrix approach for determining error field sensitivity to coil deviations,” *Plasma Physics and Controlled Fusion* **60** (2018), 10.1088/1361-6587/aab6cb.
- ²⁸N. McGreivy, S. R. Hudson, and C. Zhu, “Optimized finite-build stellarator coils using automatic differentiation,” *arXiv* (2020), 10.1088/1741-4326/abcd76, arXiv: 2009.00196.
- ²⁹V. V. Nemov, S. V. Kasilov, W. Kernbichler, and G. O. Leitold, “Poloidal motion of trapped particle orbits in real-space coordinates,” *Physics of Plasmas* **15**, 052501 (2008).
- ³⁰J. L. Velasco, I. Calvo, S. Mulas, E. Sanchez, F. I. Parra, A. Cappa, and t. W.-X. team, “A model for the fast evaluation of prompt losses of energetic ions in stellarators,” *arXiv:2106.05697 [physics]* (2021), arXiv: 2106.05697.